High temperature thermoelectric properties of CoSb3 skutterudites with PbTe inclusions

Caroline Chubilleau, Bertrand Lenoir, Philippe Masschelein, Anne Dauscher, Christophe Candolfi, Emmanuel Guilmeau, Claude Godart

High temperature thermoelectric properties of $CoSb_3$ skutterudites with PbTe inclusions

C. Chubilleau[1,*], B. Lenoir[1], P. Masschelein[1], A. Dauscher[1], C. Candolfi[1], E. Guilmeau[2], C. Godart[3]

[1] Université de Lorraine, CNRS, Institut Jean Lamour, Département Chimie et Physique des Solides et des Surfaces, Ecole Nationale Supérieure des Mines de Nancy, Parc de Saurupt, F-54042 NANCY Cedex, France

[2] CRISMAT-ENSICAEN, CNRS/UMR 6508, 6 Bd Maréchal Juin, 14050, Caen Cedex, France

[3] ICMPE- CMTR, CNRS-UMR 7182, 2-8, rue H. Dunant, F-94320 THIAIS, France

* Present address: CEA/LITEN/DTNM/LCSN, CEA Grenoble, 17 rue des Martyrs, F-38054 Grenoble cedex 09, France

Corresponding author:

e-mail: anne.dauscher@ijl.nancy-universite.fr, phone: +33 383 584 170, fax: +33 383 584 344

Abstract

Nano-structured thermoelectric materials generally exhibit enhanced properties. PbTe-$CoSb_3$ thermoelectric composites (0-8 %wt of PbTe) have been successfully prepared by freeze-drying nanoparticles of PbTe (6 nm in diameter, synthesized by laser fragmentation of micron-sized particles in water) with micron-sized skutterudite $CoSb_3$ powders (~ 5 µm in diameter, synthesized by powder metallurgy), followed by spark plasma sintering. X-ray diffraction analyses and scanning electron microscopy observations have been performed.

Microstructures reveal an agglomeration of the PbTe particles at the grain boundaries of $CoSb_3$. Electrical resistivity, thermopower, and thermal conductivity measurements have been performed in the 300-800 K temperature range. The composites exhibit *n*-type conduction whereas the reference $CoSb_3$ skutterudite is *p*-type. This change of conduction mode is attributed to substitution of Sb for a minute amount of Te in the composites. The influence of both PbTe nanoparticules and Te on the thermoelectric properties is discussed in detail.

Keywords: composites, nanostructuring, skutterudites, electrical resistivity, Seebeck coefficient, thermal conductivity

1. Introduction

Energy crisis and sake of environment make energy renewable technologies aimed to be potential substitutes to fossil fuel a hot research area. Thermoelectricity can be considered as one of the attractive ways since it allows either direct conversion of heat to electricity or heat management via refrigeration. Depending on the temperature range of use and application, different families of materials prevail. For intermediate power generation applications, $CoSb_3$ skutterudite-based materials have been intensively studied because of their interesting dimensionless figure-of-merit ZT ($ZT = S^2T/\rho\kappa$ where T is the absolute temperature, S the Seeebeck coefficient or thermopower, ρ the electrical resistivity, and κ the total themal conductivity) and their good mechanical properties [1]. The binary $CoSb_3$ compound exhibits good electrical properties but fails by its too high lattice thermal conductivity (~ 10 W/mK at 300 K) [2]. To reduce significantly this parameter, different strategies have been used: (i) substitutions either on the Co or the Sb sites [3,4], (ii) and/or filling the large structural voids of the crystalline structure by one, two or even three elements with large atomic mass and small ionic radius to provide scattering of phonon of different wave-lengths [1, 5-10], (iii) and/or bulk nanostructuring in order to enhance the number of interfaces acting as effective scattering centers for the heat-carrying phonons. Nanostructuring has been realized either by introducing nanoparticles in the skutterudite matrix made of micron-sized particles [11-15], or by producing in situ precipitates [16-19] or by reducing the particle size of the matrix to nano [20--25]. The highest ZT obtained so far was reached in the triple filled n-type $Ba_{0.08}La_{0.05}Yb_{0.04}Co_4Sb_{12}$ with $ZT = 1.7$ at 850 K [11].

Current preparation methods involve classical powder metallurgy routes (ball milling for the mixing and/or the size reduction of the matrix material, melt spinning) or chemical routes, generally associated to spark plasma sintering (SPS) as the densification mean. We report

herein the synthesis and the high temperature (300 – 800 K) transport properties of PbTe-$CoSb_3$ composites. Different from previous studies is the semiconducting character of the inclusions, i.e. PbTe, and the preparation way of the composites (PbTe nanoparticles fabrication by pulsed laser fragmentation in water, ultrasonic mixing with $CoSb_3$ in ethanol, freeze-drying, SPS). Several amounts (2-8 wt%) of nano-sized PbTe have been introduced in a reference $CoSb_3$ skutterudite to investigate in detail their influence on the transport properties, and especially on the lattice thermal conductivity that is expected to be decreased.

2. Experimental details

Laser fragmentation, using a pulsed Nd:YAG laser (Continuum Powerlite Precision 8000, repetition rate = 10 Hz, output energy: 400 mJ, pulse duration: 7s, wavelength: 1064 nm), of micron-sized PbTe powders in water has been applied to produce nanosized (average diameter 6 nm) PbTe particles following a process described in detail in [26-28]. Powders have been collected after water removal by freeze-drying (FTS system EZ585, 17 mTorr, - 80 °C) during seven days. Rietveld refinement performed on the freeze-dried powders shows that the particle size is unchanged with regard to the nano-sized particles produced from laser fragmentation. Classical powder metallurgy techniques have been used to prepare the micron-sized particles of $CoSb_3$ used as the matrix [29,30]. Mixtures of $CoSb_3$ and x wt% PbTe nanopowders ($0 \leq x \leq 8$) have been ultrasonically dispersed in ethanol and freeze-dryed during one day. These composite powders have then been densified by SPS (Syntex, Dr SINTER Lab 1500) at 873 K under 50 MPa of pressure for a total experiment time of 6 min. All samples exhibit a relative density higher than 98 %, showing no influence with respect to the content of nanoparticles included [28].

X-ray powder diffraction (XRD) patterns were collected in the 2θ range of 25-80° from grinded sintered samples using a Siemens D500 spectrometer with Co $K_{\alpha 1}$ radiation. The

micromorphology of the specimens (mirror-polished and fractured) have been observed by scanning electron microscopy (FEG-SEM, Philips XL-30) in the secondary electron or back-scattered electron (BSE) modes. Electron dispersive spectroscopy analyses (EDS) and X-ray mappings have been performed to check the chemical homogeity of the samples.

Simultaneous measurements of the thermopower (S) and the electrical resistivity (ρ) were performed over the 300 – 800 K temperature range in a ZEM3-ULVAC device under partial helium atmosphere. Thermal conductivity values were obtained from measurements of thermal diffusivity (NETZSCH, LFA 427) and specific heat (NETZSCH, DSC 403 F3) both realized under argon atmosphere. For all property measurements, separate disks and bar-shaped samples (typical dimensions 2.5×2.5×10 mm^3) were sectioned from the same ingots. Note that no evidence of Pb presence has been observed on the different DSC curves, confirming that the amount of Pb in the composite samples, detected from resistivity measurements at low temperature [28], is very low.

3. Results and discussion

The XRD patterns of the sintered $CoSb_3$ + x wt% PbTe samples are displayed in Figure 1. The matrix (x = 0) is a single-phase material with a minute amount of Sb as a secondary phase. Introduction of even small amounts of PbTe leads to the appearence of additional peaks that can be attributed to PbTe. Their intensity becomes higher as the PbTe amount increases. SEM shows that PbTe is not well dispersed in the matrix. Some areas are very rich in PbTe, as can be evidenced from the magnification of the SEM images (white areas in Figs 2a, c, e), where it agglomerates at the grain boundaries. The amount of these zones increases with the PbTe content. These areas coexist with large regions where a small fraction of PbTe is present thus appearing more dispersed (white spots, Figs b,d,f) even

though the same tendency to agglomerate is still observable. The amount of the agglomarates also increases with the PbTe content. A more detailed analysis of the microstructure is given in ref 28. Similar microstructures have already been encountered in other nanostructured skutterudite materials [13,15,16,18].

The high temperature dependences of the thermoelectric power are reported in figure 3. The thermoelectric power of the reference material $CoSb_3$ is positive in the whole temperature range studied whereas it is negative for the three PbTe-$CoSb_3$ composites, suggesting a change in the mode of conduction from *p* to *n* with the addition of PbTe. Similar features had already been observed for measurements performed below room temperature [28]. It was attributed to the substitution of minute amounts of Sb for Te. All samples exhibit the same temperature dependences. The thermopower increases with temperature, in absolute values for the composites, reach a maximum, and then decreases. A maximum of 205 μV/K is attained at 520 K for the binary skutterudite and of - 290 μV/K at 400 K for the composites. The observed decrease can be attributed to the influence of minority charge carriers. When two kinds of charge carriers are involved, the thermopower can be expressed by:

$$S = \frac{S_n \sigma_n + S_p \sigma_p}{\sigma_n + \sigma_p} \qquad (1)$$

where $S_{n,p}$ and $\sigma_{n,p}$ are the partial thermopowers and electrical resistivities for the *n* and *p* type charge carriers, repectively. As the sign of S_n and S_p are opposite, the presence of minority carriers, electrons in the case of $CoSb_3$ and holes in the case of the composites, will always give rise to a decrease in *S*. Below 520 K, the composites display no clear trend upon the amount of introduced PbTe and their thermopower values are always higher than that of the reference skutterudite. According to the classical theory of semiconductors, it suggests a reduction in the charge carriers density and/or an increase in the effective mass. A modification of the scattering mechanisms could be another possible cause. Above 520 K, the

thermopower values of all composites are quite similar and, in absolute values, close to those of $CoSb_3$.

The temperature dependences of the electrical resistivity are reported in figure 4 for the four studied samples. A decrease is observed for the composites above 400 K and a sharper decrease above 520 K for $CoSb_3$, in agreement with the conlusions drawn from the thermopower. Indeed, the presence of both electrons and holes must contribute to decrease the electrical resistivity. At 780 K, all samples exhibit very close electrical resistivities, suggesting that the intrinsic regime is reached or close to be reached.

The temperature dependences of the total thermal conductivity κ are plotted in figure 5a. At room temperature, the electronic contribution κ_e, estimated from the Wiedemann-Franz law ($\kappa_e = L_0 T/\rho$, where L_0 is the Lorentz number taken to the value of a degenerate electron gas $L_0 = 2.44\ V^2K^{-2}$), represents only ≈ 2 % of the total thermal conductivity. It reaches ≈ 15 % at 800 K for both $CoSb_3$ and the composites. Until 600 K, the total thermal conductivity can be thus mainly ascribed to the lattice contribution κ_l. The thermal conductivity of $CoSb_3$ decreases with temperature until a minimum around 600 K (~ 5 $Wm^{-1}K^{-1}$) before starting to rise with temperature. This behaviour is in good agreement with literature results [31]. Supposing that the Umklapp mechanism is the main scattering source of phonons in the 300 - 600 K temperature range, the lattice thermal conductivity should vary according to a $1/T$ law. As can be seen in Fig. 5b, the temperature dependences follow this law quite well. The enhancement beyond 600 K means that another channel for heat transport is present. It may be attributed to the ambipolar contribution resulting from the presence of minority carriers, as suggested by the thermopower analyses. The ambipolar term arises from the fact that a heat flow can take place without a charge flow. Electron-hole pairs are created at the hot end by the absorption of energy from the source. These pairs move down the temperature gradient and recombine at the cold end, releasing the energy of recombination. With the simultaneous

presence of electrons and holes, the electronic thermal conductivity (κ_e) is then the sum of three contributions: electrons (κ_{el}), holes (κ_h), and electron-hole pairs ($\kappa_{el\text{-}h}$, ambipolar). It is difficult to discriminate $\kappa_{el\text{-}h}$, from κ_e since an estimation of the former is quite complex and requires the knowledge of the partial electrical conductivities of electrons and holes as well as the partial thermoelectric powers. However, as evidenced from Fig. 5b, the phononic part remains the main contribution even at 800 K. Even though no clear trend as a function of x is observed, the total thermal thermal conductivities of the composites are lower than those of $CoSb_3$. This decrease may be explained by the microstructure (presence of large defects) and/or by the substitution of Te for Sb resulting in point defect scattering, even if the Te concentration and mass fluctuations between Sb and Te are weak [32]. It is relevant to note the complex behaviour of κ versus temperature. Between 300 and 600 K, the total thermal conductivity of the composites follows the same trend as $CoSb_3$: the Umklapp mechanism manifest itself first at the lowest temperatures and then holes and electron-hole pairs start playing a role (see Fig. 5). More surprising is the behaviour above 600 K where a decrease in the thermal conductivity is observed while an increase would be expected. As the electronic thermal conductivity should increase above 600 K (likewise in $CoSb_3$), it means that an additional scattering mechanism is present to reduce strongly the lattice contribution. This point is not yet understood and requires further investigation. No anomalies could be detected on both the electrical resistivity and thermopower, suggesting that only the lattice contribution is affected. We however note that the anomaly starts at around 600K, temperature that is close to the melting point of Pb. Whether the minute amounts of liquid Pb can be held responsible for the anomalous behaviour is still an open question.

From the values of ρ, S and κ, we calculated the thermoelectric figure of merit ZT whose dependences are shown in Fig. 6 for all samples. The reference skutterudite exhibit a maximum ZT value close to 0.13 at 595 K, typical for a material whose carrier concentration

is close to 2.8×10^{18} cm^{-3}. The temperature dependences of the composites are more complex due to the wavy behaviour of the Seebeck coefficient. The maximum *ZT* is reached at 440 K for a PbTe content of 4 wt%. At this temperature, the *ZT* value is twice that reached for $CoSb_3$ following the trend observed at room temperature [28]. It is however important to keep in mind that this direct comparison is difficult to validate because of their different type of conduction. Beyond this temperature, the performance of the reference material is higher.

4. Conclusion

PbTe/$CoSb_3$ composites have been successfully prepared via an unconventional route. A clear tendency of the PbTe nanoparticles to agglomerate at the grain boundaries has been observed. The thermoelectric properties of the composites have been investigated in the 300-800 K temperature range and have been compared to the reference binary $CoSb_3$ skutterudite. An unexpected change of conductivity type with respect to the reference sample $CoSb_3$ occurred in the composites and has been attributed to minute substitution of Sb for Te. The particular features observed at temperatures roughly higher than 600 K reflect the presence of minority carriers. No clear trend upon the rate of introduced PbTe on the properties is observed. The reduction of the thermal conductivity observed in the composites with regard to $CoSb_3$ may be due to both point defect scattering and nanostructuration. An anomaly in the thermal conductivity of the composites above 600 K was evidenced. The figure of merit *ZT* of the composites is higher until a temperature of 440 K at which it becomes twice higher than that of the binary compounds. Unfortunately, at higher temperature this beneficial effect collapses due to the particular dependences of the Seebeck coefficient.

Acknowledgments

Authors acknowledge the support by the European Network of Excellence CMA (Complex Metallic Alloys).

References

[1] Uher C (2001) Skutterudites: Prospective novel thermoelectrics. In: Tritt T (ed.) Semiconductors and Semimetals: Recent Trends in Thermoelectric Materials Research I. Academic Press, New York, 69:139

[2] Morelli DT, Meisner GP (1995) J Appl Phys 77:3777

[3] Katsuyama S, Shichijo Y, Ito M, Majima K, Nagai H (1998) J Appl Phys 84:6708

[4] Wojciechowski K, Toboła J, Leszczyñski J (2003) J Alloys Compds 361:19

[5] Sales BC (2003) Filled skutterudites. In: Gschneidner KAJ, Bünzli, J-CC, Pecharsky V (eds). Handbook on the Physics and Chemistry of the Rare Earths. North Holland: Elsevier, New York, 33:1

[6] Shi X, Yang J, Salvador JR, Chi M, Cho JY, Wang H, Bai S, Yang J, Zhang W, Chen L. (2011) J Amer Chem Soc 133:7837

[7] Bai SQ, Huang XY, Chen LD, Zhang W, Zhao XY, Zhou YF (2010) Appl Phys A 100:1109

[8] Zhao W, Wei P, Zhang Q, Dong C, Liu L, Tang X (2009) J Amer Chem Soc 131:3713

[9] Shi X, Kong H, Li CP, Uher C, Yang J, Salvador JR, Wang H, Chen L, Zhang W (2008) Appl Phys Lett 92:182101

[10] Ballikaya S, Wang G, Sun K, Uher C (2011) J Elect Mater 40:570

[11] Mi JL, Zhao XB, Zhu TJ, Tu JP (2008) Appl Phys Lett 92:029905

[12] Alboni PN, Ji X, He J, Gothard N, Hubbard J, Tritt TM (2008) J Appl Phys 103:113707

[13] Katsuyama S, Kanayama Y, Ito M, Majima K, Nagai H (2007) J Electron Mater 36:711

[14] Shi X, Chen L, Yang J, Meisner GP (2004) Appl Phys Lett 84:2301

[15] He Z, Stiewe C, Platzek D, Karpinski G, Müller E, Li S, Toprak M, Muhammed M (2007) Nanotechnol 18:1

[16] Zhao XY, Shi X, Chen LD, Zhang WQ, Bai SQ, Pei YZ, Li XY, Goto T (2006) Appl Phys Lett; 89:092121.

[17] Li H, Tang X, Zhang Q, Uher C (2009) Appl Phys Lett 94:102114

[18] Zhou C, Sakamoto J, Morelli D, Zhou X, Wang G, Uher C (2011) J Appl Phys 109:063722

[19] Eilertsen J, Rouvimov S, Subramanian MA (2012) Acta Mater 60:2178

[20] Toprak MS, Stiewe C, Platzek D, Williams S, Bertini L, Müller E, Gatti C, Zhang Y, Rowe M, Muhammed M (2004) Adv Funct Mater 14:1189

[21] Mi JL, Zhu TJ, Zhao XB, Ma J (2007) J Appl Phys 101:054314

[22] Alleno E, Chen L, Chubilleau C, Lenoir B, Rouleau O, Trichet MF, Villeroy B (2010) J Elect Mater 39:1966

[23] Li H, Tang X, Su X, Zhang Q, Uher C (2009) J Phys D: Appl Phys 42:145409

[24] Lu PX, Wu F, Han HL, Wang Q, Shen ZG, Hu X (2010) J All Comp 505:255

[25] Park KH, Kim IH (2011) J Elect Mater 40:493

[26] Kosalathip V, Dauscher A, Lenoir B, Migot S, Kumpeerapun T (2008) Appl Phys A 93:235

[27] Chubilleau C, Lenoir B, Migot S, Dauscher A (2011) J Colloid Interf Sci 357:13

[28] Chubilleau C, Lenoir B, Dauscher A, Godart C (2012) Intermetallics 22:47

[29] Puyet M, Lenoir B, Dauscher A, Pécheur P, Bellouard C, Tobola J, Hejtmanek J (2006) Phys Rev B 73:035126

[30] Puyet M, Lenoir B, Dauscher A, Weisbecker P, Clarke SJ (2004) J Solid State Chem 177:2138

[31] Sharp J, Jones EC, Williams RK, Martin PM, Sales BC (1995) J Appl Phys 78:1013

[32] M. Puyet, PhD, INPL, Nancy, 2004

Caption for figures

Figure 1

XRD patterns of spark plasma sintered (x wt%) PbTe-$CoSb_3$ composites.

Figure 2

Back-scattered electron images of the PbTe-$CoSb_3$ composites. a,b) 2 wt% PbTe., c,d) 4 wt% PbTe, e,f) 8 wt% PbTe. PbTe, as controlled by EDS analyses, appears as the white spots in the images.

Figure 3

Temperature dependences of the Seebeck coefficient S for $CoSb_3$ and the (x wt%) PbTe-$CoSb_3$ composites.

Figure 4

Temperature dependences of the electrical resistivity ρ for $CoSb_3$ and the (x wt%) PbTe-$CoSb_3$ composites.

Figure 5

Temperature dependences of the total thermal conductivity κ for $CoSb_3$ and the (x wt%) PbTe-$CoSb_3$ composites. a) as a function of T, b) as a function of $1/T$. We can note from figure b) that all samples follow a 1/T dependence below 600 K suggesting that heat transport is dominated by the lattice contribution. The deviation from the straight line represents the electronic contribution (κ_e) assuming Umklapp process only.

Figure 6

Temperature dependences of the figure of merit *ZT* for $CoSb_3$ and the (x wt%) PbTe-$CoSb_3$ composites.

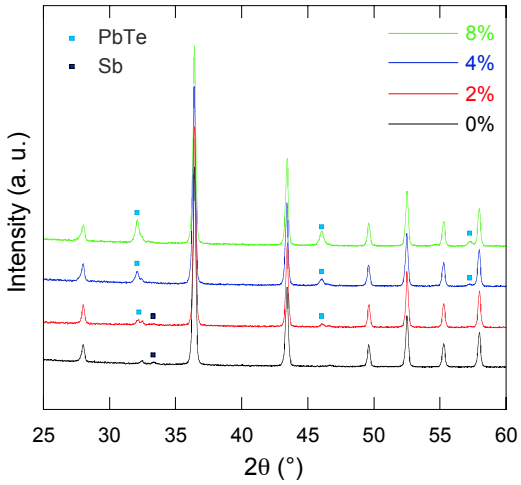

Figure 1

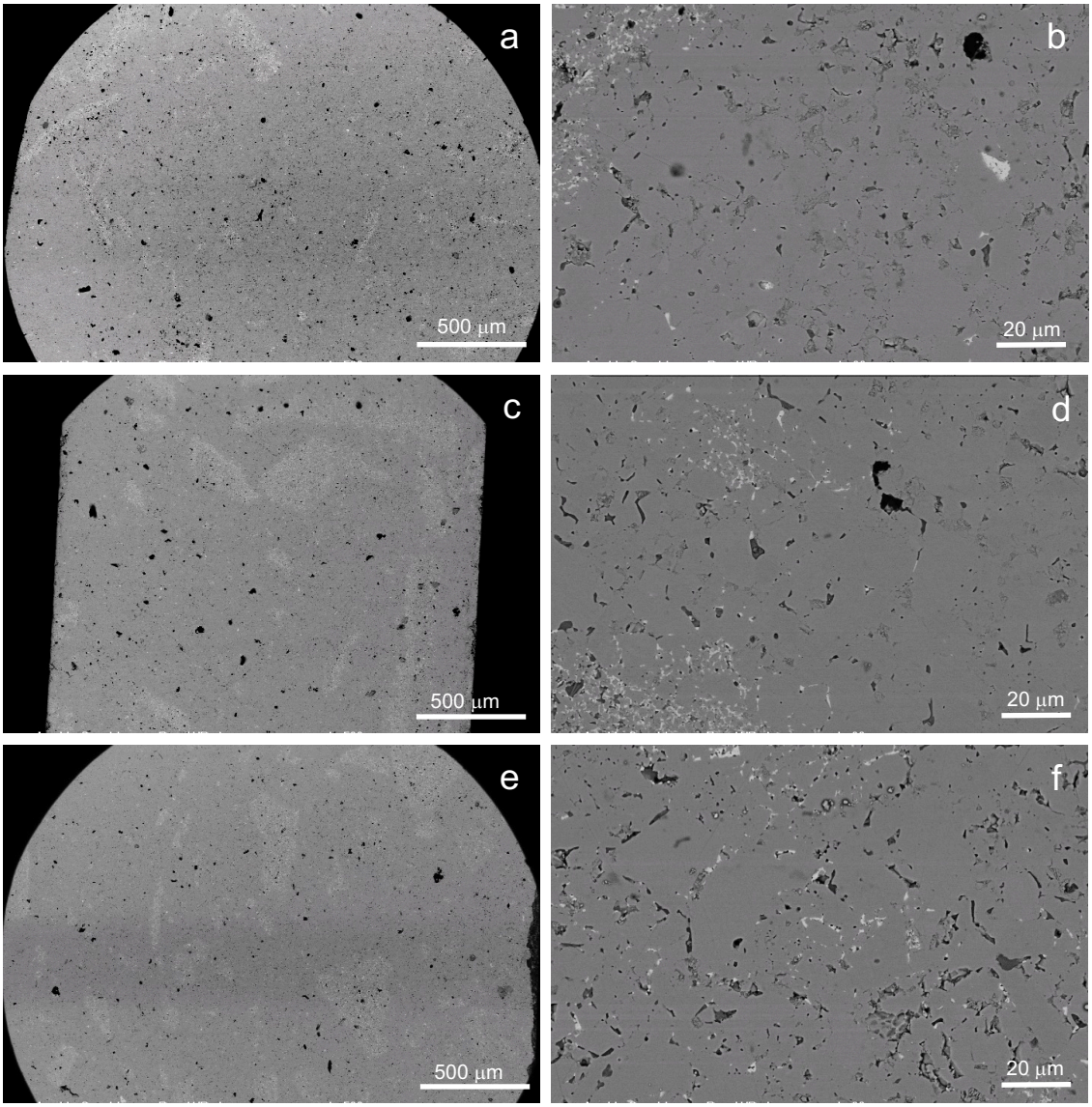

Figure 2

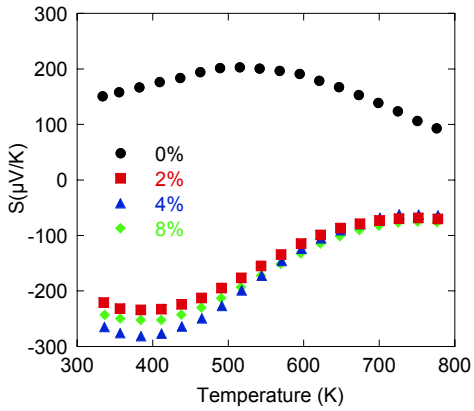
300
200
100
0
-100
-200
-300
S(μV/K)
0%
2%
4%
8%
300
400
500
600
700
800
Temperature (K)

Figure 3

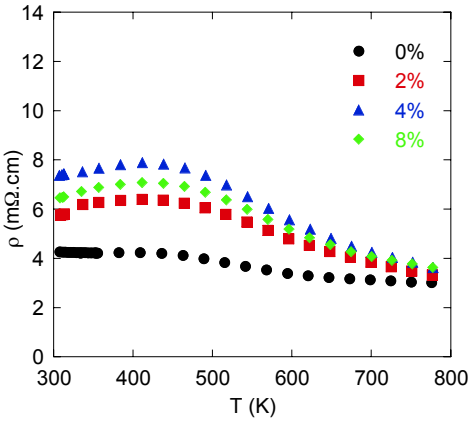

Figure 4

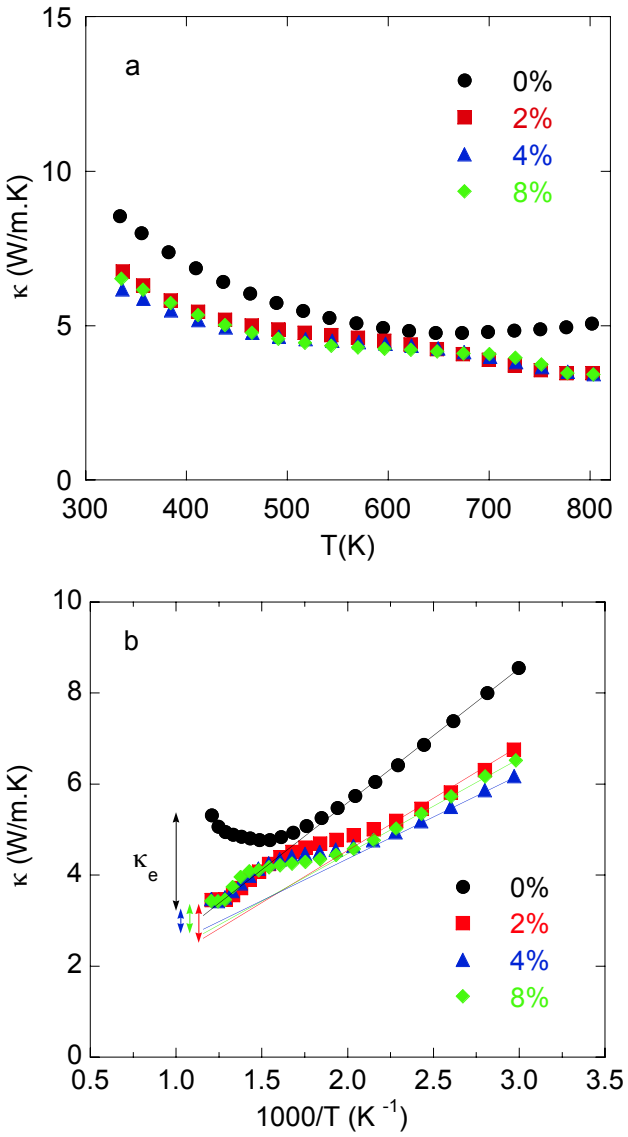

Figure 5

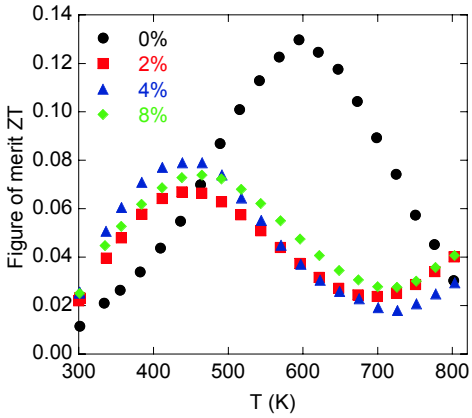
0%
2%
4%
8%
Figure of merit ZT
T (K)
0.00
0.02
0.04
0.06
0.08
0.10
0.12
0.14
300
400
500
600
700
800

Figure 6